Report

Cell Systems

In Situ Peroxidase Labeling and Mass-Spectrometry Connects Alpha-Synuclein Directly to Endocytic Trafficking and mRNA Metabolism in Neurons

Graphical Abstract

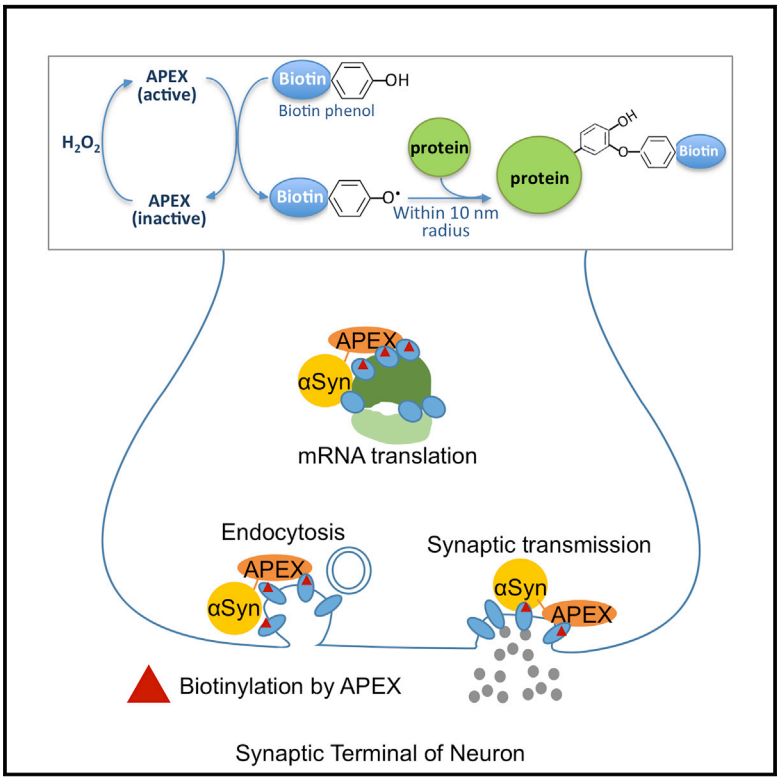

Highlights

- APEX labeling defines the protein network in the vicinity of α-syn in living neurons
- Labeled proteins: synaptic transmission, endocytosis, retromers and mRNA translation
- α-syn is proximal to many PD and other neurodegenerative disease genes
- α-syn APEX and genetic interaction maps converge on endocytosis and mRNA translation

Authors

Chee Yeun Chung, Vikram Khurana, Song Yi, ..., Marc Vidal, Alice Y. Ting, Susan Lindquist

Correspondence

cychung@yumanity.com (C.Y.C.), vkhurana@bwh.harvard.edu (V.K.)

In Brief

Chung et al. define the protein network in the vicinity of α-synuclein in living neurons using a peroxidase labeling technique coupled with mass spectrometry. α-synuclein directly interacts with proteins involved in synaptic transmission, endocytosis, retromer trafficking and mRNA translation.

Chung et al., 2017, Cell Systems *4*, 1–9
February 22, 2017
http://dx.doi.org/10.1016/j.cels.2017.01.002

CellPress

Please cite this article in press as: Chung et al., In Situ Peroxidase Labeling and Mass-Spectrometry Connects Alpha-Synuclein Directly to Endocytic Trafficking and mRNA Metabolism in Neurons, Cell Systems (2017), http://dx.doi.org/10.1016/j.cels.2017.01.002

Cell Systems
Report

In Situ Peroxidase Labeling and Mass-Spectrometry Connects Alpha-Synuclein Directly to Endocytic Trafficking and mRNA Metabolism in Neurons

Chee Yeun Chung,[1,10,11,16,*] Vikram Khurana,[1,2,3,10,*] Song Yi,[4,5,13] Nidhi Sahni,[4,5,12] Ken H. Loh,[6] Pavan K. Auluck,[1,14] Valeriya Baru,[1] Namrata D. Udeshi,[7] Yelena Freyzon,[1] Steven A. Carr,[7] David E. Hill,[4,5] Marc Vidal,[4,5] Alice Y. Ting,[6,15] and Susan Lindquist[1,8,9]

[1]Whitehead Institute for Biomedical Research, Cambridge, MA 02142, USA
[2]Ann Romney Center for Neurologic Disease, Department of Neurology, Brigham and Women's Hospital and Harvard Medical School, Boston, MA 02115, USA
[3]Harvard Stem Cell Institute, Cambridge, MA 02138, USA
[4]Center for Cancer Systems Biology (CCSB) and Department of Cancer Biology, Dana-Farber Cancer Institute, Boston, MA 02215
[5]Department of Genetics, Harvard Medical School, Boston, MA 02115, USA
[6]Department of Chemistry, Massachusetts Institute of Technology, Cambridge, MA 02142, USA
[7]The Broad Institute of MIT and Harvard, Cambridge, MA 02142, USA
[8]Department of Biology, Massachusetts Institute of Technology, Cambridge, MA 02139, USA
[9]Howard Hughes Medical Institute, Department of Biology, Massachusetts Institute of Technology, Cambridge, MA 02139, USA
[10]Co-first author
[11]Present address: Yumanity Therapeutics, Cambridge MA 02139
[12]Present address: Department of Systems Biology, The University of Texas MD Anderson Cancer Center, Houston, TX 77030, USA and Graduate Program in Structural and Computational Biology and Molecular Biophysics, Baylor College of Medicine, Houston, TX 77030, USA
[13]Present address: Department of Systems Biology, The University of Texas MD Anderson Cancer center, Houston, TX 77030
[14]Present address: Biogen, Inc. Cambridge, MA 02142
[15]Present address: Department of Genetics, Biology and Chemistry, Stanford University, Stanford, CA 94305
[16]Lead Contact
*Correspondence: cychung@yumanity.com (C.Y.C.), vkhurana@bwh.harvard.edu (V.K.)
http://dx.doi.org/10.1016/j.cels.2017.01.002

SUMMARY

Synucleinopathies, including Parkinson's disease (PD), are associated with the misfolding and mis-trafficking of alpha-synuclein (α-syn). Here, using an ascorbate peroxidase (APEX)-based labeling method combined with mass spectrometry, we defined a network of proteins in the immediate vicinity of α-syn in living neurons to shed light on α-syn function. This approach identified 225 proteins, including synaptic proteins, proteins involved in endocytic vesicle trafficking, the retromer complex, phosphatases and mRNA binding proteins. Many were in complexes with α-syn, and some were encoded by genes known to be risk factors for PD and other neurodegenerative diseases. Endocytic trafficking and mRNA translation proteins within this spatial α-syn map overlapped with genetic modifiers of α-syn toxicity, developed in an accompanying study (Khurana et al., this issue of *Cell Systems*). Our data suggest that perturbation of these particular pathways is directly related to the spatial localization of α-syn within the cell. These approaches provide new avenues to systematically examine protein function and pathology in living cells.

INTRODUCTION

Neurodegenerative diseases are characterized by the loss of distinct neuronal populations. In most of these diseases, a critical event leading to this neuronal loss is the abnormal folding and mis-trafficking of proteins. Different diseases are defined by the particular culprit proteins and the specific cell-types affected. For example, abnormal intraneuronal accumulation of the protein α-synuclein (α-syn) defines the synucleinopathies, a group of diseases that includes Parkinson's disease (PD) and dementia with Lewy bodies (DLB) (Goedert et al., 2013). In these diseases, midbrain dopaminergic and cortical glutamatergic neurons are among the neuronal populations that prominently degenerate; their degeneration is associated with clinically important phenotypes. α-syn is encoded by the *SNCA* gene. The identification in PD of mutations and polymorphisms at the *SNCA* gene locus has causally tied the misfolding of this protein to disease (Shulman et al., 2010).

αsyn is a highly abundant neuronal protein. Early studies localized α-syn predominantly to the pre-synaptic terminal (Maroteaux et al., 1988). Subsequent studies have concentrated on this synaptic localization, and its apposition to synaptic vesicles(Auluck et al., 2010). Abundant evidence now indicates that α-syn is found on the cytosolic face of vesicles and adopts an amphipathic conformation upon binding phospholipid membranes (Auluck et al., 2010; Davidson et al., 1998; Mizuno et al., 2012). Its localization to other cellular compartments, including the nucleus, remains relatively under-explored but may be relevant to disease

(Kontopoulos et al., 2006). Beyond neurons, α-syn is also abundant in other cell types, notably red blood cells (Nakai et al., 2007). While its biological function remains far from fully known, findings in cellular models from yeast to neurons have coalesced around important roles for α-syn in vesicle trafficking and synaptic physiology (Greten-Harrison et al., 2010; Chandra et al., 2005; Auluck et al., 2010; Vargas et al., 2014; Scott et al., 2010; Gitler et al., 2008). These studies have suggested that the normal physiological function of the protein is related to its cellular pathology. Thus, knowledge of α-syn localization and native interactions may also shed light on disease mechanisms when the protein misfolds and mis-traffics.

The elucidation of a protein's physical interactions can provide essential clues to its function. For α-syn, a number of complementary approaches have been used to identify around 300 physical interactions (http://thebiogrid.org/112506/summary/homo-sapiens/snca.html). First, co-immunoprecipitation has been used in conjunction with mass spectrometry to delineate diverse protein-protein associations (McFarland et al., 2008). While this methodology is unbiased and high-throughput, it depends on lysis of cells that disrupts the native cellular context. Moreover, only stable, protein complexes are recovered by standard co-immunoprecipitation techniques. Second, low-throughput candidate-based experiments have validated biochemical interactions between α-syn and numerous other proteins and demonstrated that specific interactions with α-syn are required for specific physiological functions. These include the identification of interactions between the C terminus of α-syn and SNARE proteins such as Synaptobrevin-2/VAMP2 and SNAP-25 (Sharma et al., 2012). Complemetary α-syn knockout experiments suggest a role for α-syn in SNARE complex assembly during exocytosis (Burré et al., 2014; Burré et al., 2010) and subsequent studies have extended this function to multiple steps in vesicle trafficking, including endocytosis (Vargas et al., 2014). Additional low-throughput interaction studies, including reconstitution in multi-protein complexes, have revealed biochemical interactions between α-syn and other proteins implicated in PD, including the microtubule-associated protein Tau (encoded by the MAPT gene) (Jensen et al., 1999) and Parkin (Choi et al., 2001). Finally, it is worth noting that conventional yeast-two-hybrid technologies—in which a prey and bait protein must interact in the nucleus of yeast cells for a positive readout of the assay—have been largely unsuccessful in recovering any interactions for α-syn (Engelender et al., 1999), likely because meaningful interactions for a membrane-associated protein like α-syn may critically depend on subcellular context.

In this study, we built on previous work and defined the α−syn's physiologic compartments within the cell and its protein-protein interaction network within its native environment using a chemical biology approach. In the presence of H_2O_2, ascorbate peroxidase (APEX) oxidizes numerous phenol derivatives to phenoxyl radicals. Such radicals are short-lived (<1 msec) and can covalently react with electron-rich amino acids such as Tyr within their small labeling radius (<10 nm). This chemistry combined with mass spectrometry was recently exploited to define the proteome of organelles, including the mitochondrial matrix (Rhee et al., 2013) and intermembrane space (Hung et al., 2014). The overarching advantage of this technique is that the labeling is performed when the cell is still alive, with all membranes and protein-protein interactions preserved, including transient interactions.

Rather than using the APEX tag-based methodology to define the proteome of an organelle or cellular compartment, we used it here to define the proteins in the immediate vicinity of α-syn in mammalian cells, including primary neurons. We then used two orthogonal assays (co-immunoprecipitation and membrane-2-hybrid [MYTH]; Stagljar et al., 1998) to ask whether proteins identified through APEX interacted with α-syn in physical complexes. In order to address the significance of these proteins and their functional compartments to α-syn proteotoxicity, we compared them to a comprehensive genetic network generated through unbiased genome-wide screens against α-syn toxicity (accompanying manuscript Khurana et al., this issue of *Cell Systems*). In sum, the use of multiple orthogonal approaches in this study defines the intrinsic localization and protein interaction network of α-syn, and their intimate relationship to its proteotoxicity.

RESULTS

APEX Defines the In Situ Proteome of α-syn in Neurons

We first tested the APEX-based approach for defining α-syn's protein neighborood in HEK293 cells. The data from HEK293 cells confirmed that APEX could yield useful information on the localization, neighboring proteome and protein-protein interactions of α-syn in living cells (see Figures S1 and S2 and Table S1 for complete details).

The misfolding of α-syn causes pathology in neurons, including loss of dopaminergic and cortical neurons. We thus optimized the APEX technique in this more disease-relevant cell type. We utilized primary rat cortical neurons that can be cultured in high abundance at relatively high levels of consistency and homogeneity compared to dopaminergic neurons. We used a "second-generation" APEX with improved catalytic efficiency (APEX2) (Lam et al., 2015). This has been optimized for robust labeling in live neurons when expressed under the synapsin promoter. We tagged APEX2 to the C-terminal, cytosol facing end of α−syn, allowing the enzyme to be directed to the native cellular environment of α−syn (Figure 1A).

After 10 days in culture, we transduced α-syn-APEX2 into rat primary cortical neurons using lentivirus. At this time point, endogenous α-syn is fully expressed. We have previously shown that at a multiplicity of infection (MOI) of 20, α-syn overexpression from an extremely strong CMV promoter causes overt toxicity only after 2 weeks (Chung et al., 2013). To avoid the potentially confounding effects of neurotoxicity on our proteomic analysis, we transduced neurons at an MOI of 5 and expressing α-syn from a synapsin promoter, well below toxic levels. Three days after viral transduction, we activated APEX by a short (1 min) pulse of H_2O_2 in the presence of biotin-phenol immediately prior to lysing the cells (Figure 1B).

APEX2 produced robust and specific labeling patterns in neurons. For αSyn-APEX2, this localization was punctate in neurites as expected. In contrast, nucleus-excluded APEX2 (NES-APEX2) showed diffuse cytosolic and neuritic labeling. Mito-APEX2 labeling was consistent with discrete mitochondrial localization (Figure 1C). Biotinylated proteins from αSyn-APEX2, NES-APEX2 and APEX2-negative neurons (Figure 1D) were quantified using isobaric tags for relative and absolute

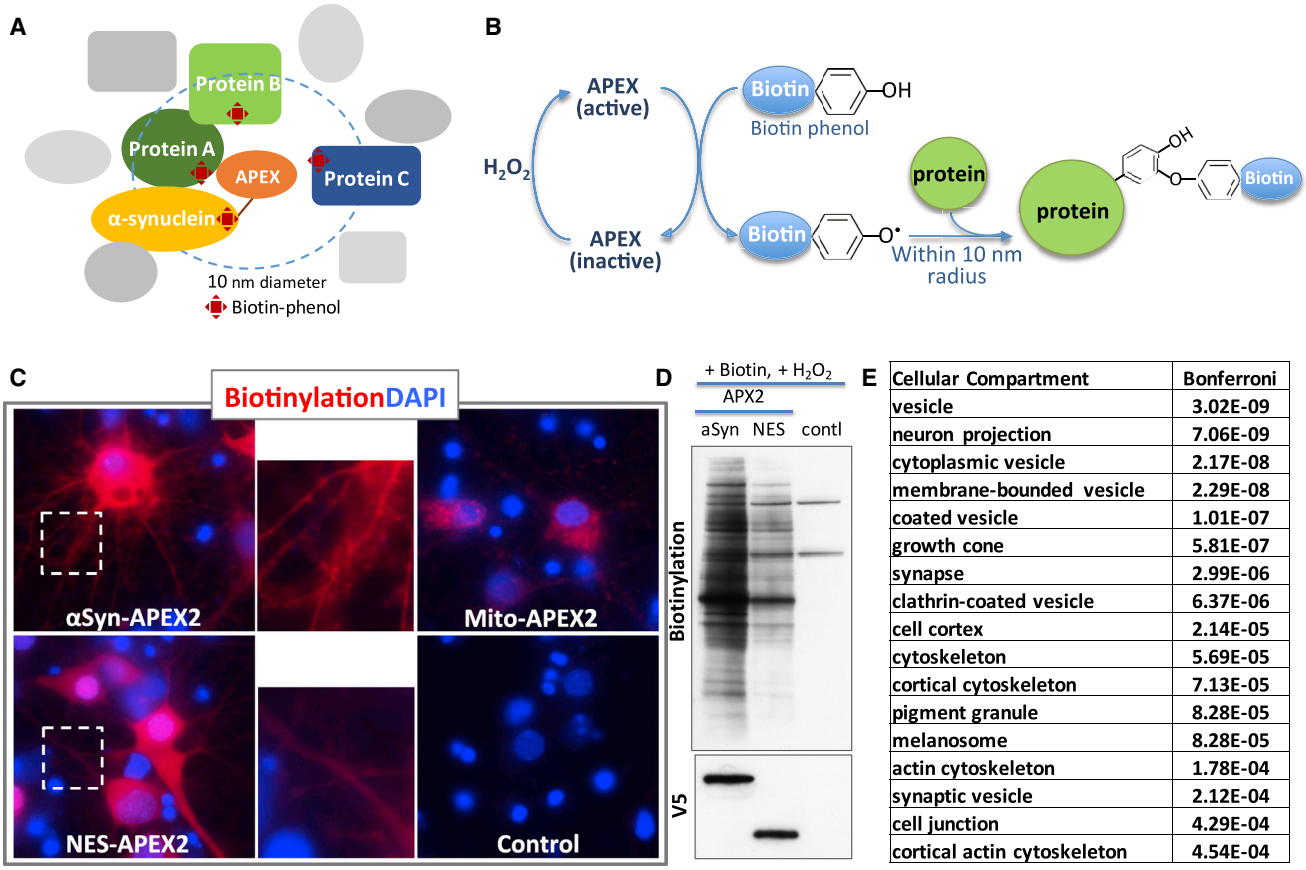

Cellular Compartment	Bonferroni
vesicle	3.02E-09
neuron projection	7.06E-09
cytoplasmic vesicle	2.17E-08
membrane-bounded vesicle	2.29E-08
coated vesicle	1.01E-07
growth cone	5.81E-07
synapse	2.99E-06
clathrin-coated vesicle	6.37E-06
cell cortex	2.14E-05
cytoskeleton	5.69E-05
cortical cytoskeleton	7.13E-05
pigment granule	8.28E-05
melanosome	8.28E-05
actin cytoskeleton	1.78E-04
synaptic vesicle	2.12E-04
cell junction	4.29E-04
cortical actin cytoskeleton	4.54E-04

Figure 1. α–syn-APEX2-Labeled Proteins in Primary Rat Cortical Neurons

(A) Schematic diagram of α−syn-APEX depicting a genetically engineered peroxidase APEX tagged to the C-terminal of wild-type α-syn. Labeled proteins are within an approximately 10nm distance of the tag. Some of these will be in complexes with α-syn.

(B) With a short pulse of H_2O_2, APEX becomes activated and creates a free radical from biotin tyramide, labeling amino acid residues of proteins in the vicinity of APEX.

(C–E) Pattern of APEX2 labeling in primary cortical neurons is distinct for α-syn-APEX2-, Mito-APEX2-, NES-APEX2-infected neurons by imaging (C) and western blot (D). Inset: distinct labeling patterns highlighted in neuritic processes. Mito: mitochondrial matrix-targeted; NES: Nuclear exclusion sequence. (E) Compartments enriched for proteins labeled in α-syn-APEX2- versus NES-APEX2 conditions (Gene ontology enrichment scores for cellular compartment; DAVID functional annotation clustering https://david.ncifcrf.gov).

quantification (iTRAQ) mass spectrometry (Figure S3). More than 2,000 proteins were identified by MS, and after filtering the dataset for nonspecific cytosolic labeling by comparing enrichment in the α-syn-APEX2 condition versus the NES-APEX2 control (see Figure S4 and STAR Methods for full details) we identified 225 enriched proteins proximal to α-syn in cortical neurons (Table S2).

Of the 225, there was enrichment for proteins in subcellular compartments previously associated with α-syn, including vesicles and the synaptic terminal (Figure 1E, Figure S5 and Table S3). Cellular processes such as protein transport and vesicle trafficking (including clathrin-mediated endocytosis and retromer-mediated retrograde trafficking) were among the top pathways enriched (Table 1).

Beyond the expected localization at the synaptic terminal and vesicle compartments, the α-syn-APEX2 analysis also implicated other compartments, pathways and processes including actin and microtubule cytoskeleton and serine/threonine-specific dephosphorylation (Table 1). The cytoskeletal proteins included the microtubule-associated protein tau (MAPT) that has been heavily implicated in distinct forms of parkinsonism. MAPT polymorphisms are independent risk factors for PD (Shulman et al., 2010), and physical interactions between MAPT and α-syn have been well described in the literature (Jensen et al., 1999). Particularly prominent classes of proteins significantly enriched among the α-syn-APEX2-labeled proteins were mRNA binding, processing, and translation proteins. These were explored in more detail below.

MYTH and Genetic Interaction Analysis Confirm a Direct Effect of α-syn on Endocytic and Retrograde Trafficking Pathways

α-syn-APEX2 prominently labeled clathrin-mediated endocytic proteins, as well as two proteins within the retromer complex that traffics proteins from endosomes to late Golgi, VPS29 and VPS35. These are pathways and proteins that have been strongly implicated in human studies of PD. Indeed, the *VPS35* gene is also known as the *PARK17* locus because mutation of

Table 1. Biological Processes Enriched for Proteins Labeled in α-syn-APEX2 versus NES-APEX2

Biological Process	No.	Genes	Bonferroni
Membrane trafficking	9	SYP, RAB3A, SYT1, CPLX2, RAB3B, RAB8A, COPB1, RAB6A, DNM1	4.03E-10
Protein transport	27	VPS29, RAB3A, XPO1, RAB3B, RAB3C, AP1B1, NAPG, AP2B1, STX12, TRIM3, COPB1, VPS35, STAM, RAB6A, TNPO2, SEC24C, RAB8A, SCAMP3, ACTN4,	2.67E-09
Transport	45	VPS29, RAB3A, XPO1, CPLX2, RAB3B, OSBP, ATP1B1, CPLX1, RAB3C, NAPG, AP1B1, CACNB1, CACNB3, ATP6V1B2, AP2B1, STX12, TRIM3, COPB1, VPS35, PAFAH1B1, STAM, SV2B, RAB6A, TNPO2, SEC24C, SCAMP3, RAB8A, ACTN4, RAB4B, G3BP2, ATP1A1, RPH3A, HNRNPA1, CADPS, AP2A2, RABEP1, VCP, LASP1, RAB35, TXN, KHSRP, RAB15, ATP6V0A1, OSBPL11, ERC1	2.65E-06
Endocytosis	8	PACSIN1, AP2A2, RABEP1, AP1B1, SYNJ1, DNM1, SH3GL2, SH3GL1	1.76E-02
Cytoskeleton	29	SHROOM2, TLN1, ACTR3B, WASF1, ABI2, ABI1, ARPC4, CTNNB1, TPM3, CTTN, PFN2, CRMP1, MAPT, PAFAH1B1, ACTN1, DCTN3, DCTN2, PPP1R9B, LASP1, MAP2, TMOD2, SPTBN2, SPTBN1, MAPRE1, ERC2, SEPT6, DNM1, ADD2, SPTAN1	4.03E-08
Actin-binding	16	SHROOM2, ACTN4, ACTR3B, WASF1, ACTN1, ARPC4, TPM3, PPP1R9B, PFN2, SYN1, LASP1, TMOD2, SPTBN2, SPTBN1, ADD2, SPTAN1	1.51E-05
Microtubule	12	SHROOM2, MAP1LC3A, DYNLL2, MAPT, KIF5C, MAP2, PAFAH1B1, ARPC4, MAPRE1, MAPRE3, DNM1, DCTN2	8.99E-03
Serine/threonine-specific phosphatase	5	PPP1CA, PPP3CB, PPP3CA, PPP1CC, PPP1CB	3.65E-04
RNA-binding	19	XPO1, RNMT, SYNJ1, HNRNPA2B1, G3BP2, SYNCRIP, ILF3, CDC5L, HNRNPA1, HNRNPR, DDX17, TIA1, HTATSF1, KHSRP, CIRBP, PABPC1, MARS, HNRNPAB, DDX42	4.47E-03
Protein biosynthesis	10	EIF3C, EIF3D, CARS, EEF1B2, DARS, EIF3L, EEF2, RPS10, EEF1D, MARS	4.37E-02

Protein trafficking, transport and endocytosis were the top category labeled by α-syn-APEX2. In addition, cytoskeleton (actin and microtubule), protein phosphatases and mRNA metabolism (RNA binding and protein synthesis) are the processes that are labeled by α-syn-APEX2.
Gene ontology enrichment scores for biological process; DAVID functional annotation clustering https://david.ncifcrf.gov.

its coding sequences causes Mendelian PD (Zimprich et al., 2011; Hunn et al., 2015).

The APEX2 data alone cannot distinguish whether α-syn was simply located in the endocytic and retrograde trafficking compartments, or if it was bound in macromolecular complexes to these proteins. So, for each protein in the endocytic or retrograde trafficking pathway that emerged in our APEX dataset, we performed a binary α-syn interaction assay with membrane yeast two-hybrid (MYTH, see STAR Methods, Figure S2 and Table S5). We tested all isoforms available in the ORFeome for 19 endocytosis/retromer proteins suggested by APEX. Of these, 10/19 were positive with MYTH. These included Clathrin, Dynamin, and VPS29 (Figure 2A, Table S5). Another retromer-associated protein, SNX1, also formed a complex with α−syn (Figure 2A) but the closely related retromer proteins, VPS35 and SNX5, did not. Our data suggests that α-syn impacts endocytic and retrograde trafficking through direct physical interactions with key proteins in these pathways.

While α-syn-APEX2 in conjunction with MYTH can uncover physical interactions between proteins, as noted above, complementary genetic approaches are required to reveal the biological significance of these interactions. In an accompanying manuscript (Khurana et al., 2017, this issue), we executed three genome-wide screens in yeast to identify genes that impact α-syn toxicity. Homologs of a number of human PD genes, including VPS35, were recovered in these screens. Loss of VPS35 enhances α-syn toxicity, confirmed here for a strain that expresses moderately toxic levels of α-syn (IntTox) (Figure 2B). The convergence of both physical and genetic interaction data on the same protein complexes substantiates these direct interactions between α-syn and its neighboring proteins as inciting events in α-syn toxicity.

Our genetic screens did not recover the two other core retromer components, *VPS26* or *VPS29*, as modifiers of α-syn toxicity. However, high-throughput screens are never comprehensive. In this case, the identification of VPS29 in our spatial assays (α-syn-APEX2 and MYTH) led us to test the effects of deleting each of the retromer genes on α-syn toxicity in a candidate-based experiment. In fact, deletion of VPS26 or VPS29 also enhanced α-syn toxicity (Figure 2B). Thus, these independent genetic and physical interaction analyses were mutually reinforcing and complementary. In this case, the retromer emerges as a multi-protein complex that interacts physically with α-syn and plays a key role in its toxicity. These connections to α-syn and its toxicity provide important biological context for *VPS35 (PARK17)* as a PD gene. Figure S6 shows an adaptation of the entire endocytosis pathway from the Kegg database demonstrating the substantial data linking this pathway to α-syn in both our genetic (red star) and spatial (green for APEX2; yellow for MYTH) analyses.

Convergence of Genetic and Spatial Maps on Vesicle Trafficking and mRNA Translation

Taking our lead from the retromer-α-syn interaction, we looked more broadly at the relationship of genetic modifiers of α-syn toxicity to the spatial α-syn-APEX2 map. In the accompanying manuscript, we developed computational methods that could assemble genetic modifiers of α-syn toxicity into molecular

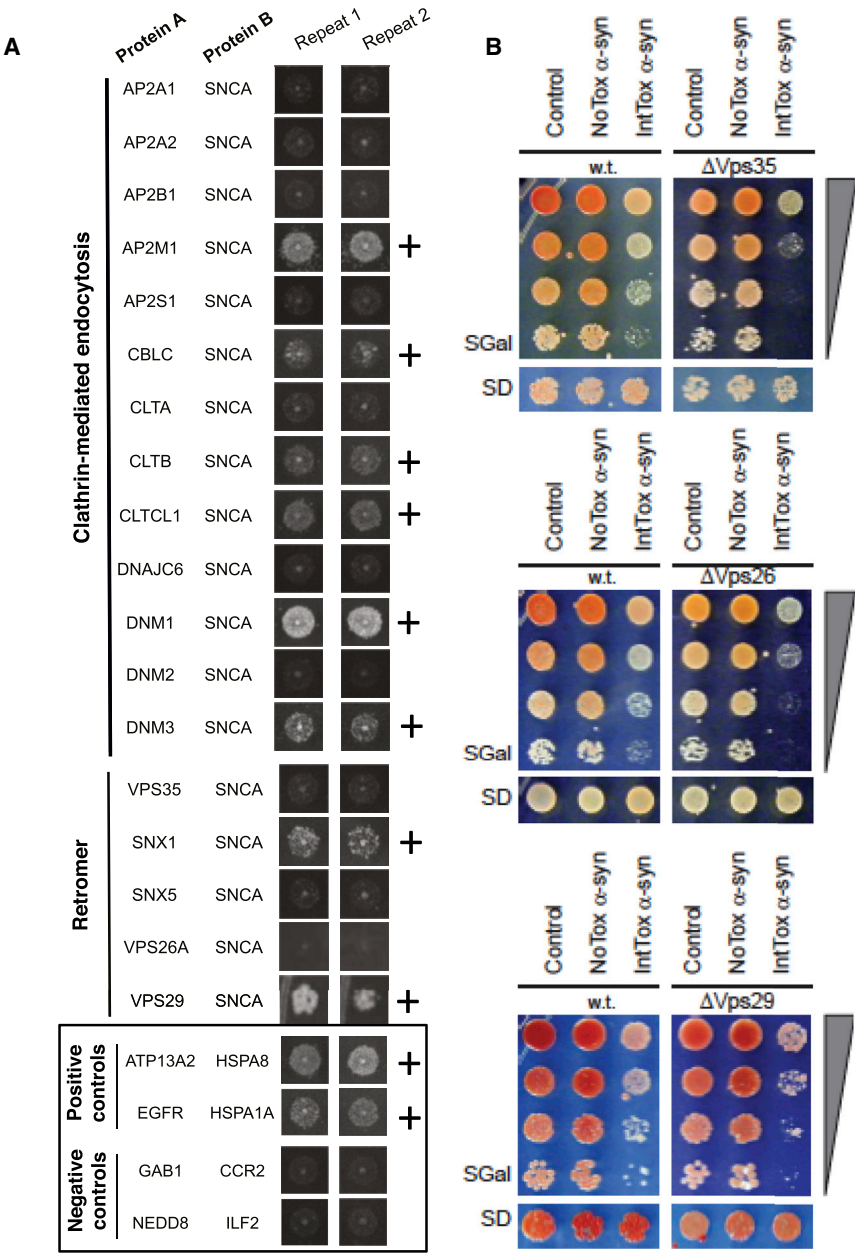

Figure 2. Endocytic and Retromer Trafficking Proteins Interact with α-syn Physically and Genetically

(A) Endocytic and retromer trafficking proteins enriched in α-syn-APEX2-labeled neurons are tested for physical interaction with a-syn using the membrane-2-hybrid (MYTH) technique (Figure S2). Interactions scored as positive are marked "+." Positive and negative controls are shown in the box.

(B) Spotting assays on yeast agar plates indicate that deleting each of the three core retromer components (VPS26, VPS29 and VPS35) enhances toxicity in a strain expressing moderately toxic levels of α-syn (IntTox) but does not enhance toxicity in Control or NoTox α-syn yeast strains.

networks and place these networks squarely in the context of the human proteome. This network is represented in Figure 3A. Many core components of the genetic network encode proteins that our α-syn-APEX2 and MYTH analysis revealed were in the immediate vicinity of α-syn (Figure 3A, filled circles). Beyond the retromer complex, these include proteins involved in other trafficking steps (RAB6A, Synaptojanin/SYNJ1), mRNA translation factors and other mRNA binding proteins (PABPC1, G3BP1/2,TIA1/TIAL1), signaling proteins and phosphatases (Calcineurin/PPP3C, PPP1C).

The overlap between genetic and spatial maps extends beyond these specific proteins. For example, while the spatial map identified α-syn in the immediate vicinity of Rps10, the genetic map identified multiple other small ribosomal protein complex components as genetic modifiers. Likewise, while many EIF3 subunit components emerged from the spatial map, other translation initiation factors (including PABPC1, EIF4G1 and ATXN2) emerged in the genetic map. Indeed, there was a convergence of the genetic and spatial maps at the pathway enrichment level (DAVID functional annotation clustering https://david.ncifcrf.gov), particularly for vesicle trafficking ($p = 4.03E-10$; and mRNA translation/binding proteins ($p = 4.47E-03$; Figure 3A and Table S4). Of the mRNA translation hits in the APEX neuron study, 5 were available for testing by MYTH in the ORFeome library. Of these, 4/5 were confirmed (EIF3C, EIF3L, RPS12 and PABPC1; Figure 3B; Table S5 and Figure S7). These data imply that, as for vesicle trafficking proteins, mRNA translation and binding proteins are proximal interactors with α-syn that are integrally involved in its mechanisms of toxicity. This was also supported by the results from our accompanying paper, where we identified a defect in mRNA translation in PD patient-dervied neurons (Khurana et al., in this issue).

It is worth noting that, while the genetic map of α-syn toxicity was generated in yeast, the spatial α-syn-APEX map was established in mammalian neurons. While the yeast genetic map was "humanized" (that is, placed in the context of the human proteome), a number of important relationships would likely be missed, most likely for proteins that are neuron-specific. This indeed was the case. For example, the spatial α−syn map recovered multiple RAB3 proteins. These are neuron-specific RAB proteins involved in synaptic vesicle exocytosis and do not feature among our genetic screen hits in yeast. However, multiple previous studies, including from our own lab, have established that modulating the levels of these RAB proteins can modify α-syn toxicity in neurons, shown for both RAB3A (Gitler et al., 2008) and RAB3B (Chung et al., 2009).

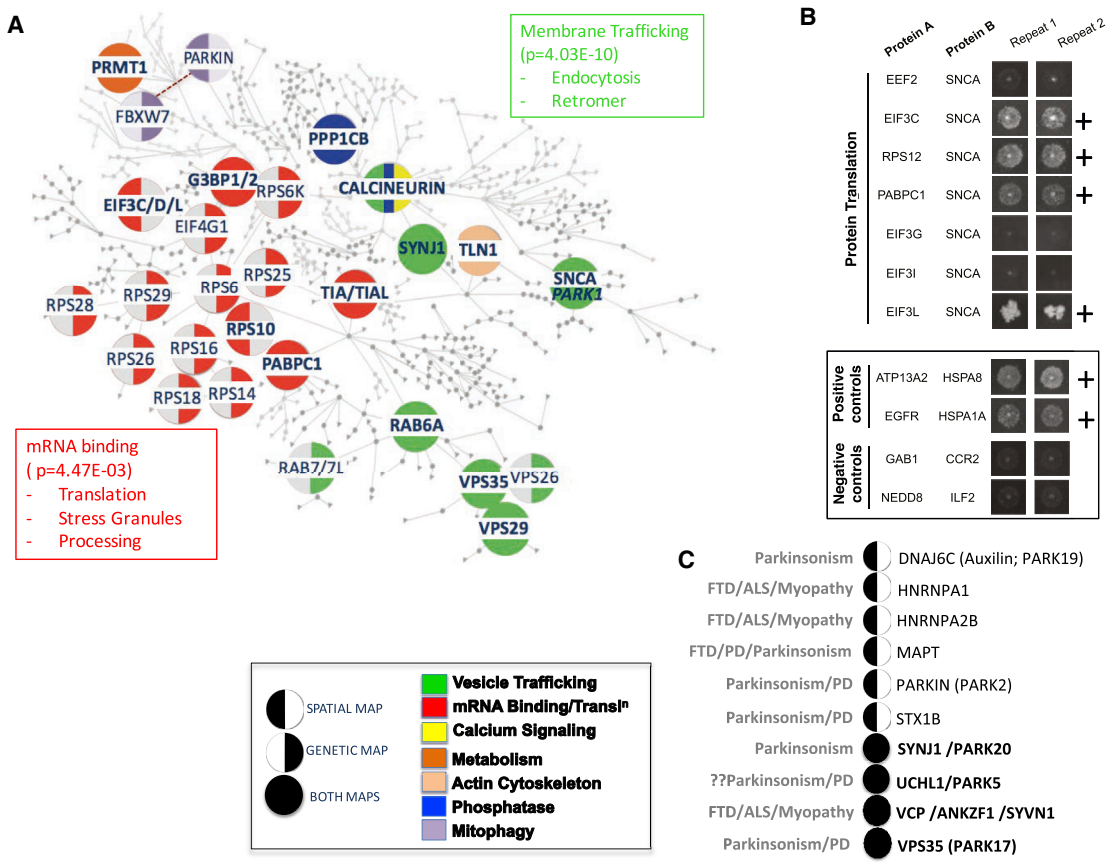

Figure 3. Convergence of Genetic Interaction Map and Spatial—α-syn-APEX2-Labeled—Map on Vesicle Trafficking and mRNA Metabolism

(A) α-syn-APEX2-labeled proteins are overlaid on to a "humanized" genetic interaction network map. Each circular node of the genetic network depicts a human protein related to a genetic modifier of α-syn toxicity in yeast (full details in Khurana et al., 2017, this issue), or an α-syn-APEX2-labeled protein that is in a complex with a genetic hit. Enlargement of certain nodes is purely for emphasis and readability. Nodes that belong to both the genetic and α-syn-APEX2 maps are indicated fully shaded. These include G3BP1/2, TIA/TIAL1, PABPC1, VPS29, vPS35, RAB6A, PPP1CB, PPP3C (Calcineurin), TLN1 (Talin 1) and PRMT (Protein Arginine Methyl Transferase). Nodes that were only recovered as genetic modifiers are marked with a left semi-circle. Conversely, nodes that were only recovered in the spatial α-syn-APEX2 map are indicated with a right semi-circle. Pathways/processes that are enriched in both genetic and spatial maps include vesicle trafficking, mRNA metabolism and mRNA binding proteins and phosphatases (Gene ontology enrichment scores for cellular compartment; DAVID functional annotation clustering https://david.ncifcrf.gov).

(B) mRNA translation-related proteins are tested for physical interaction with α-syn using the membrane-2-hybrid (MYTH) technique. Interactions scored as positive are marked "+." Positive and negative controls are shown in the box.

(C) Neurodegenerative disease-associated genes emerge among α-syn-APEX2-labeled proteins. Some of these are also recovered in the genetic network of α-syn toxicity modifiers (Khurana et al., 2017; full circles). Others are not (left semi-circle). VCP was among the α-syn-APEX2-labeled proteins. While VCP was not directly recovered as a genetic modifier of α-syn toxicity, two proteins that work closely with VCP in endoplasmic reticulum- and mitochondria-associated degradation - SYVN1 and ANKZF1 - were recovered in genetic screens. Notably, a gene no longer considered a PD gene (*UCHL1/PARK5*) was recovered in both the spatial and genetic α-syn maps.

Finally, another measure of the biological significance of our spatial α-syn map comes from human genetic studies. Our genetic and spatial maps converged on specific human neurodegenerative disease genes (Figure 3C), including two Mendelian parkinsonism genes, *VPS35 (PARK17)* (Zimprich et al., 2011) and *SYNJ1 (PARK20*) (Quadri et al., 2013; Olgiati et al., 2014; Krebs et al., 2013). Also recovered in the spatial map was *PARKIN (PARK2)*. While *PARKIN* does not have a direct yeast homolog, a related ubiquitin ligase in yeast, Cdc4 (FBXW7) (Ivatt et al., 2014; Ekholm-Reed et al., 2013), was recovered in our genetic screens. A third *PARK* gene, *DNAJC6 (PARK19)* (Köroğlu et al., 2013; Olgiati et al., 2015; Edvardson et al., 2012), was recovered in the spatial map. DNAJC6 is also known as an auxilin, and is a chaperone involved in clathrin uncoating. One *PARK* gene that is no longer considered a bona fide PD gene because of failure to replicate in human genetic studies is *UCHL1 (PARK5).* It appeared in both our genetic and spatial maps, suggesting that it may be involved in α-syn toxicity. In fact, a number of mechanistic studies have previously suggested such a relationship (Cartier et al., 2012; Liu et al., 2009; Yasuda et al., 2009) and this association may be of relevance in the broader context of synuclein pathology beyond PD. Beyond Mendelian risk factors, our spatial map further recovered two neuronal genes implicated through common variants in PD, *MAPT* and Syntaxin 1B (*STX1B*) (Nalls et al., 2014). Finally, like VCP, two other proteins related to multisystem proteinopathies, were recovered in our spatial map,

including HNRNPA1 and HNRNPA2B (Müller-Kuller et al., 2015; Taylor 2015; Kim et al., 2013). These findings collectively deepen our understanding of α-syn toxicity, and specifically establish a key relationship between the native cellular context of the α-syn protein in neurons to pathogenic mechanisms of high relevance to human disease.

DISCUSSION

How the intrinsic localization of a misfolding protein relates to its proteotoxicity has been unclear. The major advance of the APEX2 labeling methodology is its ability to capture the localization of a protein and its proteome context within a living cell. It provides a snapshot of proteins, somewhat analogous to immunocytochemistry, except that APEX2 provides information at proteome-scale that is independent of the idiosyncrasies of immunohistochemistry. In short, APEX2 captures subcellular complexity and spatial context. This is not captured by techniques that require cell lysis, like co-IP, or with heterologous systems such as MYTH, in which a bait protein is tethered to the ER membrane. However, APEX2 will also label proteins that are in the vicinity of the tagged protein, but not necessarily complexed to it directly. It is also important to point out that the APEX2 tag could impede protein-protein interactions or the entry of the tagged protein to specific subcellular compartments. Moreover, proteins without surface-accessible Tyr or other electron-rich residues will not be detected with the APEX technique. These different methodologies are thus complementary. When they are convergent, they are mutually reinforcing. When they are divergent, interactions are worthy of investigation with yet additional methods.

At a high level, this study and the accompanying work (Khurana et al., 2017) systematically explore α-syn toxicity through a variety of complementary, independent methodologies: physical and spatial mapping techniques like APEX2 and MYTH, multiple genetic screens, computational tools, and functional validation in patient-derived neurons. Proteins that emerge in common between these approaches, proximal as they are to α-syn itself, are likely to reflect direct and inciting events in α-syn cytotoxicity. These include vesicle trafficking proteins (RAB6A, VPS35, SYNJ1), mRNA translation factors (PABPC1) and key signaling molecules (PPP3/Calcineurin). The correlation with entirely independent human genetic studies reinforces the significance of these proteins and pathways to human disease. Most broadly, the building of molecular networks with our various approaches provides a view of how seemingly disparate genes, proteins and pathways interconnect to cause proteotoxicity.

While these methods are powerful, they clearly do not replace deeper, mechanistic studies or studies in more complex models. For example, in the accompanying study the emergence of mRNA translation factors in our spatial and genetic networks allowed us to uncover new pathologic phenotypes in patient-derived neurons. Hence, the main strength of these studies is to identify important directions for future investigations. While mechanistic work within a neuronal context is required for a more detailed understanding of clinical observations, our studies provide a systems-level view of how intrinsic biology might relate to the pathology of misfolded and mis-trafficked proteins. These approaches can now be applied to other proteinopathies in which a relationship of intrinsic biology to disease pathology may well emerge as a common theme.

STAR★METHODS

Detailed methods are provided in the online version of this paper and include the following:

- KEY RESOURCES TABLE
- CONTACT FOR REAGENT AND RESOURCE SHARING
- EXPERIMENTAL MODEL AND SUBJECT DETAILS
- METHOD DETAILS
  - In Situ Biotin Labeling of αSyn Interactors Using αSyn-APEX
  - Rat Primary Cortical Cultures
  - Virus Production
  - Mass Spectrometry to Identify Biotinylated Proteins in HEK Cells
  - iTRAQ Mass Spectrometry for Rat Primary Cortical Neurons
  - Anti-GFP Antibody Crosslinking and Co-immunoprecipitation
  - Membrane Yeast Two Hybrid
  - Immunostaining
  - Yeast Spotting Assays
- QUANTIFICATION AND STATISTICAL ANALYSIS
  - The Quantification of the Membrane-2 Hybrid
  - p Value for Figure 1 and Table 1

SUPPLEMENTAL INFORMATION

Supplemental Information includes 7 figures and 5 tables and can be found with this article online at http://dx.doi.org/10.1016/j.cels.2017.01.002.

AUTHOR CONTRIBUTIONS

Conceptualization: C.Y.C., V.K., and S.L.; Methodology: C.Y.C., V.K., S.Y., N.S., N.D.U., and K.H.L.; Investigation: C.Y.C., V.K., S.Y., N.S., P.K.A., V.B., and Y.F.; Resources: K.H.L. and A.Y.T.; Writing-Original Draft and review and editing: C.Y.C., V.K., and S.L.; Supervision: C.Y.C, V.K., S.L., A.Y.T., D.E.H., M.V., and S.A.C.

ACKNOWLEDGMENTS

Research was supported by an HHMI Collaborative Innovation Award (V.K., C.Y.C., A.Y.T., and S.L.), the JPB Foundation (V.K., C.Y.C., S.L.), NIH K01AG038546 (C.Y.C.), HG001715 (M.V. and D.E.H), an American Brain Foundation and Parkinson's Disease Foundation Clinician-Scientist Development Award (V.K.), the Harvard Neurodiscovery Center Pilot Project Program (V.K.), the Multiple System Atrophy Coalition (V.K.), the Eleanor Schwartz Charitable Foundation (S.L.). We thank P. Thiru, B. Yuan and E. Spooner from the Whitehead Institute for expert assistance. We dedicate this manuscript to Dr Susan Lindquist—our incomparable mentor and colleague—who passed away while this manuscript was in its final stages of revision. V.K., C.Y.C., and S.L. are scientific co-founders of Yumanity Therapeutics, a company focused on developing neurodegenerative disease therapeutics.

Received: January 12, 2016
Revised: August 5, 2016
Accepted: December 15, 2016
Published: January 25, 2017

REFERENCES

Auluck, P.K., Caraveo, G., and Lindquist, S. (2010). α-Synuclein: membrane interactions and toxicity in Parkinson's disease. Annu. Rev. Cell Dev. Biol. *26*, 211–233.

Burré, J., Sharma, M., Tsetsenis, T., Buchman, V., Etherton, M.R., and Südhof, T.C. (2010). Alpha-synuclein promotes SNARE-complex assembly in vivo and in vitro. Science *329*, 1663–1667.

Burré, J., Sharma, M., and Südhof, T.C. (2014). α-Synuclein assembles into higher-order multimers upon membrane binding to promote SNARE complex formation. Proc. Natl. Acad. Sci. USA *111*, E4274–E4283.

Cartier, A.E., Ubhi, K., Spencer, B., Vazquez-Roque, R.A., Kosberg, K.A., Fourgeaud, L., Kanayson, P., Patrick, C., Rockenstein, E., Patrick, G.N., and Masliah, E. (2012). Differential effects of UCHL1 modulation on alpha-synuclein in PD-like models of alpha-synucleinopathy. PLoS ONE *7*, e34713.

Chandra, S., Gallardo, G., Fernández-Chacón, R., Schlüter, O.M., and Südhof, T.C. (2005). Alpha-synuclein cooperates with CSPalpha in preventing neurodegeneration. Cell *123*, 383–396.

Choi, P., Golts, N., Snyder, H., Chong, M., Petrucelli, L., Hardy, J., Sparkman, D., Cochran, E., Lee, J.M., and Wolozin, B. (2001). Co-association of parkin and alpha-synuclein. Neuroreport *12*, 2839–2843.

Chung, C.Y., Koprich, J.B., Hallett, P.J., and Isacson, O. (2009). Functional enhancement and protection of dopaminergic terminals by RAB3B overexpression. Proc. Natl. Acad. Sci. USA *106*, 22474–22479.

Chung, C.Y., Khurana, V., Auluck, P.K., Tardiff, D.F., Mazzulli, J.R., Soldner, F., Baru, V., Lou, Y., Freyzon, Y., Cho, S., et al. (2013). Identification and rescue of α-synuclein toxicity in Parkinson patient-derived neurons. Science *342*, 983–987.

Davidson, W.S., Jonas, A., Clayton, D.F., and George, J.M. (1998). Stabilization of alpha-synuclein secondary structure upon binding to synthetic membranes. J. Biol. Chem. *273*, 9443–9449.

Edvardson, S., Cinnamon, Y., Ta-Shma, A., Shaag, A., Yim, Y.I., Zenvirt, S., Jalas, C., Lesage, S., Brice, A., Taraboulos, A., et al. (2012). A deleterious mutation in DNAJC6 encoding the neuronal-specific clathrin-uncoating co-chaperone auxilin, is associated with juvenile parkinsonism. PLoS ONE *7*, e36458.

Ekholm-Reed, S., Goldberg, M.S., Schlossmacher, M.G., and Reed, S.I. (2013). Parkin-dependent degradation of the F-box protein Fbw7β promotes neuronal survival in response to oxidative stress by stabilizing Mcl-1. Mol. Cell. Biol. *33*, 3627–3643.

Engelender, S., Kaminsky, Z., Guo, X., Sharp, A.H., Amaravi, R.K., Kleiderlein, J.J., Margolis, R.L., Troncoso, J.C., Lanahan, A.A., Worley, P.F., et al. (1999). Synphilin-1 associates with alpha-synuclein and promotes the formation of cytosolic inclusions. Nat. Genet. *22*, 110–114.

Gitler, A.D., Bevis, B.J., Shorter, J., Strathearn, K.E., Hamamichi, S., Su, L.J., Caldwell, K.A., Caldwell, G.A., Rochet, J.C., McCaffery, J.M., et al. (2008). The Parkinson's disease protein alpha-synuclein disrupts cellular Rab homeostasis. Proc. Natl. Acad. Sci. USA *105*, 145–150.

Goedert, M., Spillantini, M.G., Del Tredici, K., and Braak, H. (2013). 100 years of Lewy pathology. Nat. Rev. Neurol. *9*, 13–24.

Greten-Harrison, B., Polydoro, M., Morimoto-Tomita, M., Diao, L., Williams, A.M., Nie, E.H., Makani, S., Tian, N., Castillo, P.E., Buchman, V.L., and Chandra, S.S. (2010). αβγ-Synuclein triple knockout mice reveal age-dependent neuronal dysfunction. Proc. Natl. Acad. Sci. USA *107*, 19573–19578.

Hung, V., Zou, P., Rhee, H.W., Udeshi, N.D., Cracan, V., Svinkina, T., Carr, S.A., Mootha, V.K., and Ting, A.Y. (2014). Proteomic mapping of the human mitochondrial intermembrane space in live cells via ratiometric APEX tagging. Mol. Cell *55*, 332–341.

Hunn, B.H.M., Cragg, S.J., Bolam, J.P., Spillantini, M.G., and Wade-Martins, R. (2015). Impaired intracellular trafficking defines early Parkinson's disease. Trends Neurosci. *38*, 178–188.

Ivatt, R.M., Sanchez-Martinez, A., Godena, V.K., Brown, S., Ziviani, E., and Whitworth, A.J. (2014). Genome-wide RNAi screen identifies the Parkinson disease GWAS risk locus SREBF1 as a regulator of mitophagy. Proc. Natl. Acad. Sci. USA *111*, 8494–8499.

Jensen, P.H., Hager, H., Nielsen, M.S., Hojrup, P., Gliemann, J., and Jakes, R. (1999). alpha-synuclein binds to Tau and stimulates the protein kinase A-catalyzed tau phosphorylation of serine residues 262 and 356. J. Biol. Chem. *274*, 25481–25489.

Khurana, V., Peng, J., Chung, C.Y., Auluck, P.K., Fanning, S., Tardiff, D.F., Bartels, T., Koeva, M., Eichhorn, S.W., Benyamini, H., et al. (2017). Genome-Scale Networks Link Neurodegenerative Disease Genes to α-Synuclein through Specific Molecular Pathways. Cell Syst. *4*, http://dx.doi.org/10.1016/j.cels.2016.12.011.

Kim, H.J., Kim, N.C., Wang, Y.D., Scarborough, E.A., Moore, J., Diaz, Z., MacLea, K.S., Freibaum, B., Li, S., Molliex, A., et al. (2013). Mutations in prion-like domains in hnRNPA2B1 and hnRNPA1 cause multisystem proteinopathy and ALS. Nature *495*, 467–473.

Kontopoulos, E., Parvin, J.D., and Feany, M.B. (2006). Alpha-synuclein acts in the nucleus to inhibit histone acetylation and promote neurotoxicity. Hum. Mol. Genet. *15*, 3012–3023.

Köroğlu, Ç., Baysal, L., Cetinkaya, M., Karasoy, H., and Tolun, A. (2013). DNAJC6 is responsible for juvenile parkinsonism with phenotypic variability. Parkinsonism Relat. Disord. *19*, 320–324.

Krebs, C.E., Karkheiran, S., Powell, J.C., Cao, M., Makarov, V., Darvish, H., Di Paolo, G., Walker, R.H., Shahidi, G.A., Buxbaum, J.D., et al. (2013). The Sac1 domain of SYNJ1 identified mutated in a family with early-onset progressive Parkinsonism with generalized seizures. Hum. Mutat. *34*, 1200–1207.

Lam, S.S., Martell, J.D., Kamer, K.J., Deerinck, T.J., Ellisman, M.H., Mootha, V.K., and Ting, A.Y. (2015). Directed evolution of APEX2 for electron microscopy and proximity labeling. Nat. Methods *12*, 51–54.

Liu, Z., Meray, R.K., Grammatopoulos, T.N., Fredenburg, R.A., Cookson, M.R., Liu, Y., Logan, T., and Lansbury, P.T., Jr. (2009). Membrane-associated farnesylated UCH-L1 promotes alpha-synuclein neurotoxicity and is a therapeutic target for Parkinson's disease. Proc. Natl. Acad. Sci. USA *106*, 4635–4640.

Maroteaux, L., Campanelli, J.T., and Scheller, R.H. (1988). Synuclein: a neuron-specific protein localized to the nucleus and presynaptic nerve terminal. J. Neurosci. *8*, 2804–2815.

McFarland, M.A., Ellis, C.E., Markey, S.P., and Nussbaum, R.L. (2008). Proteomics analysis identifies phosphorylation-dependent alpha-synuclein protein interactions. Mol. Cell. Proteomics *7*, 2123–2137.

Mizuno, N., Varkey, J., Kegulian, N.C., Hegde, B.G., Cheng, N., Langen, R., and Steven, A.C. (2012). Remodeling of lipid vesicles into cylindrical micelles by α-synuclein in an extended α-helical conformation. J. Biol. Chem. *287*, 29301–29311.

Müller-Kuller, U., Ackermann, M., Kolodziej, S., Brendel, C., Fritsch, J., Lachmann, N., Kunkel, H., Lausen, J., Schambach, A., Moritz, T., and Grez, M. (2015). A minimal ubiquitous chromatin opening element (UCOE) effectively prevents silencing of juxtaposed heterologous promoters by epigenetic remodeling in multipotent and pluripotent stem cells. Nucleic Acids Res. *43*, 1577–1592.

Nakai, M., Fujita, M., Waragai, M., Sugama, S., Wei, J., Akatsu, H., Ohtaka-Maruyama, C., Okado, H., and Hashimoto, M. (2007). Expression of alpha-synuclein, a presynaptic protein implicated in Parkinson's disease, in erythropoietic lineage. Biochem. Biophys. Res. Commun. *358*, 104–110.

Nalls, M.A., Pankratz, N., Lill, C.M., Do, C.B., Hernandez, D.G., Saad, M., DeStefano, A.L., Kara, E., Bras, J., Sharma, M., et al.; International Parkinson's Disease Genomics Consortium (IPDGC); Parkinson's Study Group (PSG) Parkinson's Research: The Organized GENetics Initiative (PROGENI); 23andMe; GenePD; NeuroGenetics Research Consortium (NGRC); Hussman Institute of Human Genomics (HIHG); Ashkenazi Jewish Dataset Investigator; Cohorts for Health and Aging Research in Genetic Epidemiology (CHARGE); North American Brain Expression Consortium (NABEC); United Kingdom Brain Expression Consortium (UKBEC); Greek Parkinson's Disease Consortium; Alzheimer Genetic Analysis Group (2014). Large-scale meta-analysis of genome-wide association data identifies six new risk loci for Parkinson's disease. Nat. Genet. *46*, 989–993.

Olgiati, S., De Rosa, A., Quadri, M., Criscuolo, C., Breedveld, G.J., Picillo, M., Pappatà, S., Quarantelli, M., Barone, P., De Michele, G., and Bonifati, V.

(2014). PARK20 caused by SYNJ1 homozygous Arg258Gln mutation in a new Italian family. Neurogenetics *15*, 183–188.

Olgiati, S., et al. (2015). DNAJC6 mutations associated with early-onset Parkinson's disease. Ann. Neurol.

Quadri, M., Fang, M., Picillo, M., Olgiati, S., Breedveld, G.J., Graafland, J., Wu, B., Xu, F., Erro, R., Amboni, M., et al.; International Parkinsonism Genetics Network (2013). Mutation in the SYNJ1 gene associated with autosomal recessive, early-onset Parkinsonism. Hum. Mutat. *34*, 1208–1215.

Rhee, H.W., Zou, P., Udeshi, N.D., Martell, J.D., Mootha, V.K., Carr, S.A., and Ting, A.Y. (2013). Proteomic mapping of mitochondria in living cells via spatially restricted enzymatic tagging. Science *339*, 1328–1331.

Scott, D.A., Tabarean, I., Tang, Y., Cartier, A., Masliah, E., and Roy, S. (2010). A pathologic cascade leading to synaptic dysfunction in alpha-synuclein-induced neurodegeneration. J. Neurosci. *30*, 8083–8095.

Sharma, M., Burré, J., Bronk, P., Zhang, Y., Xu, W., and Südhof, T.C. (2012). CSPα knockout causes neurodegeneration by impairing SNAP-25 function. EMBO J. *31*, 829–841.

Shulman, J.M., De Jager, P.L., and Feany, M.B. (2010). Parkinson's Disease: Genetics and Pathogenesis. Annu. Rev. Pathol.

Stagljar, I., Korostensky, C., Johnsson, N., and te Heesen, S. (1998). A genetic system based on split-ubiquitin for the analysis of interactions between membrane proteins in vivo. Proc. Natl. Acad. Sci. USA *95*, 5187–5192.

Taylor, J.P. (2015). Multisystem proteinopathy: intersecting genetics in muscle, bone, and brain degeneration. Neurology *85*, 658–660.

Udeshi, N.D., Mertins, P., Svinkina, T., and Carr, S.A. (2013). Large-scale identification of ubiquitination sites by mass spectrometry. Nat. Protoc. *8*, 1950–1960.

Vargas, K.J., Makani, S., Davis, T., Westphal, C.H., Castillo, P.E., and Chandra, S.S. (2014). Synucleins regulate the kinetics of synaptic vesicle endocytosis. J. Neurosci. *34*, 9364–9376.

Yasuda, T., Nihira, T., Ren, Y.R., Cao, X.Q., Wada, K., Setsuie, R., Kabuta, T., Wada, K., Hattori, N., Mizuno, Y., and Mochizuki, H. (2009). Effects of UCH-L1 on alpha-synuclein over-expression mouse model of Parkinson's disease. J. Neurochem. *108*, 932–944.

Zimprich, A., Benet-Pagès, A., Struhal, W., Graf, E., Eck, S.H., Offman, M.N., Haubenberger, D., Spielberger, S., Schulte, E.C., Lichtner, P., et al. (2011). A mutation in VPS35, encoding a subunit of the retromer complex, causes late-onset Parkinson disease. Am. J. Hum. Genet. *89*, 168–175.

STAR★METHODS

KEY RESOURCES TABLE

REAGENT or RESOURCE	SOURCE	IDENTIFIER
Antibodies		
Streptavidin conjugated Alexa Fluor 568	Thermo Fisher	S11226; RRID: AB_2315774
Avidn-horseradish peroxidase (HRP)	Vector Laboratories	A-2004; RRID: AB_2336507
Chemicals, Peptides, and Recombinant Proteins		
Biotin Phenol (tyramide)	Alice Ting	
Hoechst 33342	Thermo Fisher	62249
Experimental Models: Organisms/Strains		
Yeast strain: NMY51, *MAT**a** his3delta200 trp1-901 leu2-3,112 ade2 LYS2::(lexAop)4-HIS3 ura3::(lexAop)8-lacZ (lexAop)8-ADE2 GAL4.*	Dualsystms Biotech AG, Schlieren, Switzerland	N/A
Yeast strain: W303 *MATa can1-100, his3-11,15, leu2-3,112, trp1-1, ura3-1, ade2-1*	Susan Lindquist Laboratory	N/A
Recombinant DNA		
Lentivirus Synapsin promoter with NES-APEX2	Alice Ting lab	N/A
Lentivirus Synapsin promoter with Mito-APEX2	Alice Ting lab	N/A
Lentivirus Synapsin promoter with αSyn-APEX2	This paper	

CONTACT FOR REAGENT AND RESOURCE SHARING

Further information and requests for resources and reagents should be directed to the Lead Contact, Chee Yeun Chung cychung@yumanity.com.

EXPERIMENTAL MODEL AND SUBJECT DETAILS

Yeast strains for membrane 2 hybird: The genotype of the host yeast strain NMY51 (Dualsystems Biotech AG, Schlieren, Switzerland) is *MAT**a** his3delta200 trp1-901 leu2-3,112 ade2 LYS2::(lexAop)4-HIS3 ura3::(lexAop)8-lacZ (lexAop)8-ADE2 GAL4.*

Yeast strains for overexpression genetics: The yeast strains used were in the w303 background (MATa can1-100, his3-11,15, leu2-3,112, trp1-1, ura3-1, ade2-1). The NoTox α-syn strain contained α-syn fused to green fluorescent protein (α-syn-GFP) inserted at the his locus (pAG303Gal-α-syn-GFP). IntTox strain contained multiple tandem copies of α-syn-GFP inserted at the his and trp loci (pRS303GAL-α-syn-GFP, pRS304GAL-α-syn-GFP). IntTox strains have 4-5 copies of α-syn.

METHOD DETAILS

In Situ Biotin Labeling of αSyn Interactors Using αSyn-APEX

The labeling protocol was modified from the recent publication by Rhee et al. Genetically engineered APEX was tagged to the C-terminal of αSyn under the CMV promoter. For HEK293T cells grown in DMEM with 10% fetal bovine serum, the plasmid carrying αSyn-APEX was transiently transfected using lipofectamine 2000 (Life Technologies). 24-48 hr after transfection for HEK293T, cells were incubated in 500 μM biotin tyramide dissolved in Optimem for 30 min at 37°C. H_2O_2 was added at a final concentration of 1 mM for exactly 1 min at room temperature by washing the cells twice with PBS containing quenching reagents (5 mM Trolox, 10 mM ascorbic acid and 10 mM NaN3) for 30 s and another two washes with PBS. For a control sample for the pull down, αSyn-APEX was omitted. As for the rat primary neurons, lentivirus with synapsin promoter carrying αSyn-APEX2, NES-APEX2, mito-APEX2 was transduced at a multiplicity of infection 5. 3 days post-transduction, neurons were labeled the same way as described above. For washing, the same solution except NaN3 was used. After the final wash, cells were either fixed with 4% paraformaldehyde for immunofluorescent staining or lysed with RIPA buffer (50 mM Tris-HCl pH 7.4, 150 mM NaCl, 1% Triton x-100, 0.5% Sodium deoxycholate, 0.1% SDS and 1 mM EDTA) with protease inhibitor cocktail (Sigma) on ice for 20 min. Lysates were centrifuged for 20 min at 10,000 xg at 4°C. Supernatant was collected and protein concentration was measured using the BCA assay. Biotinylation in the samples were detected by western blot followed by probing with horseradish peroxidase-conjugated avidin (Vector Laboratories). For immunocytochemistry, Streptavidin conjugated AlexaFluor 568 (Thermo Fisher Scientific) was used. For mass spectrometry experiments, 1∼2 mg of protein was incubated with 200 μL of streptavidin magnetic bead (Pierce) slurry for 1 hr at room temperature. Beads were washed by rocking for 5 min in RIPA buffer containing 400 mM NaCl for two times, once with 1M KCl, once with 0.1 Na carbonate (pH 11.5),

twice with 2M Urea, and twice with RIPA. After the final wash, beads were boiled for 5 min in 60 μL of 1X LDS buffer (Life Technologies) + 1X reducing agent (Life Technologies) for HEK cells. The denatured solution was loaded into gel for mass spectrometry analysis. As for the primary rat cortical neurons, beads right after washing were given for further processing at Broad Institute for mass spectrometry.

Rat Primary Cortical Cultures

Embryos were harvested by cesarean section from anesthetized pregnant Sprague-Dawley rats at embryonic day 18. Cerebral cortices were isolated and dissociated with Accumax digestion for 20 min at 37°C and triuration with Pasteur pipette. Poly-ornithine and lamin-coated 96 well plates or 8 well-chambered coverglass (Lab-Tek; 70378-81) were seeded with $4x10^4$ or $8x10^4$ cells respectively in neurobasal medium (Life Technologies) supplemented with B27 (Life Technologies), 0.5 mM glutamine, 25 μM β–mercaptoethanol, penicillin (100 IU/ml) and streptomycin (100 μg/ml). One third of the medium was changed every 3 to 4 days.

Virus Production

Lentiviral constructs were packaged into virus via lipid-mediated transient transfection of the expression constructs and packaging plasmids (pMD2.G and psPAX2) to 293 cells. Lentivirus was purified and concentrated using Lenti-X Maxi Purification kit and LentiX Concentrator (Clontech) according to the manufacturer's protocol. Lentivirus titer was determined using QuickTiter Lentivirus titer kit (Lentivirus- Associated HIV p24; Cell Biolabs) according to the manufacturer's protocol.

Mass Spectrometry to Identify Biotinylated Proteins in HEK Cells

Sample Preparation

Proteins were separated by 4%–12% Nupage gels and visualized by SimplyBlue SafeStain (Life Technologies). Protein bands were excised from each lane encompassing the entire molecular weight range. The resulting bands were divided into ~2 mm squares and washed overnight in 50% methanol/ water. These were washed once more with 47.5/47.5/5% methanol/water/acetic acid for 2 hr, dehydrated with acetonitrile and dried in a speed-vac. Reduction and alkylation of disulfide bonds was then carried out by the addition of 30 μL 10 mM dithiothreitol (DTT) in 100 mM ammonium bicarbonate for 30 min to reduce disulfide bonds. The resulting free cysteine residues were subjected to an alkylation reaction by removal of the DTT solution and the addition of 100 mM iodoacetamide in 100 mM ammonium bicarbonate for 30 min to form carbamidomethyl cysteine. These were then washed with aliquots of acetonitrile, 100 mM ammonium bicarbonate and acetonitrile and dried in a speed-vac. The bands were enzymaticly digested by the addition of 300 ng of trypsin in 50 mM ammonium bicarbonate to the dried gel pieces ratio of mg trypsin for 10 min on ice. Depending on the volume of acrylamide, excess ammonium bicarbonate was removed or enough was added rehydrate the gel pieces. These were allowed to digest overnight at 37°C. The resulting peptides were extracted by the addition of 50 μL (or more if needed to produce supernatant) of 50 mM ammonium bicarbonate with gentle shaking for 10 min. The supernatant from this was collected in a 0.5 mL conical autosampler vial. Two subsequent additions of 47.5/47/5/5 acetonitrile/water/formic acid with gentle shaking for 10 min were performed with the supernatant added to the 0.5 mL autosampler vial. Organic solvent was removed and the volumes were reduced by to 15 μL using a speed vac for subsequent analyses.

Chromatographic Separations

Digestion extracts were analyzed by reversed phase high performance liquid chromatography (HPLC) using a Waters NanoAcquity HPLC and autosampler and a ThermoFisher LTQ linear ion trap mass spectrometer using a nano flow configuration. A 20 mm x 180 μm column packed with 5 μm Symmetry C18 material (Waters) using a flow rate of 15 μL per minute for two minutes was used to trap and wash peptides. These were then eluted onto the analytical column which was a self-packed with 3 micron Jupiter C18 material (Phenomenex) in a fritted 10 cm x 75 μm fused silica tubing pulled to a 5 micron tip. The gradient was isocratic 1% A Buffer for 1 min 250 nL min^{-1} with increasing B buffer concentrations to 15% B at 15 min, 27% B at 27 min and 40% B at 24.5 min. The column was washed with high percent B and re-equilibrated between analytical runs for a total cycle time of approximately 50 min. Buffer A consisted of 1% formic acid in water and buffer B consisted of 1% formic acid in acetonitrile. (Alternatively, a linear gradient of 1% to 40% B from time 1 min to time 24.5 min is used as an alternative for very low level samples where staining indicates a single band.)

Mass Spectrometry and Analysis

The mass spectrometer was operated in a dependent data acquisition mode where the five most abundant peptides detected in full scan mode were subjected to daughter ion fragmentation. A running list of parent ions was tabulated to increase the number of peptides analyzed throughout the chromatographic run. Peptides were identified from the MS data using SEQUEST algorithms that searched a species-specific database generated from NCBI's non-redundant (nr.fasta) database. Sequest filters used for indication of a positive peptide identification were: XCorr versus Charge State = 1.5, 2.00, 2.50; Sp – Preliminary Score = 500. Two peptides were required for a protein to be considered a positive identification. Data interpretation from all bands was aided by the Scaffold (Proteome Software).

iTRAQ Mass Spectrometry for Rat Primary Cortical Neurons

On-Bead Digestion

Two biological replicates of proteins enriched with magnetic streptavidin beads were washed 2x with 200 ul of 50mM Tris-HCl buffer (pH 7.5), transferred into new 1.5 mL Eppendorf tubes, and washed 2 more times with 2 M urea/50 mM Tris (pH 7.5) buffer. Following

the washes, beads were incubated for 1 hr at room temperature with 0.4 ug trypsin in 80 ul of 2 M urea/50mM Tris buffer with 1 mM DTT, while shaking at 1000xg. After the pre-digestion, 80 ul of supernatant were transferred into a new tube. Beads were washed 2x with 60 ul of 2M urea/50 mM Tris buffer, and these washes were combined with the supernatant. The eluates were spun down at 5000xg for 1 min and the supernatant was transferred into a new tube, and reduced with 4 mM DTT for 30 min at room temperature, while shaking. Following reduction the eluents were alkylated with 10 mM iodoacetamide for 45 min in the dark at room temperature, while shaking. An additional 0.5 ug of trypsin was added and samples were digested overnight at room temperature, while shaking. Following overnight digestion, samples were acidified (pH < 3) with neat formic acid, to a final concentration of 1% FA. Samples were spun down and de-salted on C18 stage tips as previously described (Udeshi et al., 2013).

Isobaric Tags for Relative and Absolute Quantification Labeling for Quantitative Proteomics

De-salted peptides were labeled with iTRAQ (4-plex) reagents in accordance with the manufacturing instructions (Sciex, Foster City, CA). Briefly, peptides were re-suspended in 30 ul of dissolution buffer, and immediately combined with 70 ul of ethanol. One unit of iTRAQ reagent was used to label each experimental condition in the 4-plex cassette. Samples were labeled as follows. Replicate 1 and 2: 114-Control, 115-NES, 116-α-Synuclein. Samples were incubated for 1 hr at room temperature with gentle shaking. Following incubation, approximately 3% of sample by volume was taken to test label incorporation. The remaining iTRAQ labeling reaction was quenched with 10 ul of 1M Tris-HCl (pH 8) for 10 min at room temperature, with gentle shaking. In a given replicate differentially labeled samples were combined, dried in a SpeedVac concentrator, and de-salted on C18 stage tips as described above.

Mass Spectrometry Analysis

De-salted peptides were re-suspended in 9 ul of 3% MeCN/0.1% FA, and analyzed by online nanoflow liquid chromatography tandem mass spectrometry (LC-MS/MS) using a Q Exactive mass spectrometer (Thermo Fisher Scientific) coupled on-line to Proxeon Easy-nLC 1000 (Thermo Fisher Scientific). Four microliters of re-suspended samples were loaded onto a microcapillary column (360 μm outer diameter x 75 μm inner diameter), which contained an integrated electrospray emitter tip (10 μm), packed to approximately 22 cm with ReproSil-Pur C18-AQ 1.9 μm beads (Dr. Maisch GmbH) and heated to 50°C. The HPLC Solvent A was 0.1% FA, and Solvent B was 90% MeCN/0.1% FA. Sample peptides were eluted into the mass spectrometer at a flow rate of 200 nl/min. The time frame of the LC-MS/MS method used was 150 min inject-to-inject with a linear gradient of 0.3%B/min, followed by a ramp to 60% B (10% B/min). The Q Exactive was operated in the data-dependent mode acquiring HCD MS/MS scans (R = 17,500) after each MS1 scan (R = 70,000) on the top 12 most abundant ions using an MS1 target of 3×10^6 and an MS2 target of 5×10^4. The maximum ion time utilized for MS/MS scans was 120 ms; the HCD-normalized collision energy was set to 27; the dynamic exclusion time was set to 20 s, and the peptide match and isotope exclusion functions were enabled.

Data Analysis

Collected data were analyzed using Spectrum Mill software package v5.0 pre-release (Agilent Technologies, Santa Clara, CA). Nearby MS scans with the similar precursor m/z were merged if they were within ± 60 s retention time, and ± 1.4 m/z tolerance. If MS/MS spectra were not within 750-4000 Da precursor MH+ range, or had sequence tag length > 0, they were excluded from the search parameters. MS/MS spectra were searched against UniProt Rat complete isoform database, which contain common laboratory contaminants. Fixed modifications included carbamidomethylation, and iTRAQ labeling of N-terminal, and internal lysines. Set variable modifications were N-terminal acetylation, and methionine oxidation. Minimum matched peak intensity was set to 30%, with pre-cursor mass tolerance of ± 20 ppm. Individual spectra were automatically assigned a confidence score using Spectrum Mill autovalidation module. Score at the peptide mode was based on target-decoy false discovery rate (FDR) of 1%. Relative abundances of proteins were determined using iTRAQ reporter ion intensity ratios from each MS/MS spectrum and the median ratio is calculated from all MS/MS spectra contributing to a protein subgroup in whole proteome samples. To account for differences in total protein amount in between samples within one iTRAQ 4-plex experiment, all iTRAQ ratios were normalized for the global population median. Proteins identified by at least 2 distinct peptides and ratio counts were considered for the dataset. We selected the proteins based on the adjusted p values and the logFC (fold change) value. Adjusted p value for the ratio of αSyn/Control and αSyn/NES was less or equal to 0.25. The ratio between αSyn and NES was considered in an attempt to avoid the non-specific cytosolic labeling that may occur "in-transit" to the final destination by αSyn-APEX. The logFC value of αSyn/control was greater than 0.2 and αSyn/NES value, greater than 0.1. These criteria were applied to maximize the inclusion of neuronal proteins that are well-demonstrated to be an αSyn interactors by low throughput methods i.e., SNAP25, MAPT, RAB3A, SYN1, SYP and SNCB.

Anti-GFP Antibody Crosslinking and Co-immunoprecipitation

Antibody Crosslinking

~110 μl Biorad AffiPrep Protein A beads were equilibrate into PBST, washed 3 times and resuspended in 500 μl PBST. 55 μg of affinity-purified rabbit anti GFP antibody (Generous gift from Dr Iain Cheesman) was mixed into the beads PBST slurry and rotated for 1hr at room temperature. The antibody attached beads were washed 3 times with PBST and 3 times with 0.2 M sodium borate, pH9. After the final wash, 900 μl of the 0.2M sodium borate, pH 9 was added to bring the final volume to ~1 ml. Freshly prepared 100 μl of 220 mM dimethylpimelimidate (Sigma) was added to the tube and rotated gently at room temperature for 30 min. Beads were washed 2 times with 0.2M ethanolamine 0.2M NaCl pH 8.5 and left rotating in the same buffer for 1 hr at room temperature to inactivate the residual crosslinker.

Co-immunoprecipitation

HEK cells expressing either GFP or αSyn-GFP were lysed with nondenaturing lysis buffer (20 mM Tris HCl pH 8, 137 mM NaCl, 1% Triton X-100 and 2 mM EDTA). The lysate was rotated for 30 min at 4°C and centrifuged at 10,000 xg for 20 min at 4°C. Supernatant

was collected and protein concentrations determined using BCA assay. ~400 μg of lysate was incubated with 50 μL anti-GFP antibody crosslinked beads for 4 hr at 4°C. Beads were washed 4 times with nondenaturing lysis buffer and denatured by boiling for 5 min in 2X LDS buffer. Supernatant was run in SDS-PAGE for western blot analysis.

Membrane Yeast Two Hybrid

This assay was used for testing protein interactions involving membrane-associated proteins and soluble cytosolic proteins. The genotype of the host yeast strain NMY51 (Dualsystems Biotech AG, Schlieren, Switzerland) is *MAT**a** his3delta200 trp1-901 leu2-3,112 ade2 LYS2::(lexAop)4-HIS3 ura3::(lexAop)8-lacZ (lexAop)8-ADE2 GAL4.* The bait vector pGBT3-STE harboring TF-Cub-Bait and the prey vector pGPR3-N harboring Nub-Prey were both transformed into the strain NMY51, while the control constructs of either Nubi-Ost1 or NubG-Ost1 was transformed together with the bait vector to serve as a positive or negative control, respectively. Successful co-transformation of both bait and prey plasmids were verified by yeast cell growth on the synthetic complete (SC) medium depleted of Leu and Trp (SC-Leu-Trp). Protein interactions were then identified by challenging yeast cells on the SC medium depleted of Leu, Trp and His, but supplemented with 10 mM of 3-amino-1,2,4-triazole (3AT), to test for *HIS3* reporter expression. In the positive control, the growth in the presence of both Cub-bait and Nub-prey indicates both proteins are expressed and correctly inserted into the membrane. In the negative control, a lack of growth in the presence of the non-interacting pair bait-Ost1 indicates that the bait protein is not an auto-activator. Prior to experimentation, to minimize inherent leaky *HIS3* expression, co-transformants of bait with Nub-Ost1 were streaked out on SC-Leu-Trp-His medium containing increasing amounts of 3-AT. The amount of 3-AT was determined that can abolish growth in the negative control (bait-NubG-Ost1), but support growth in the positive control (bait-Nubi-Ost1).

Immunostaining

Immunofluorescent labeling of human cells followed standard protocols. Briefly, cells were fixed in 4% paraformaldehyde (Electron Microscopy Sciences), blocked in 10% normal donkey serum (Jackson ImmunoResearch) for 1 hr. Primary antibody was applied overnight at 4°C. Appropriate conjugated AlexaFluor (Molecular Probes, Life Technologies) secondary antibodies were used (488, 594, 647). Hoechst 33342 (Life Technologies) was used as a nuclear stain for some studies. Imaging of cells on plastic surfaces was with an inverted epifluorescence microscope (Eclipse Ti, Nikon Instruments). These images were visualized and processed with the NIS-Elements AR software package (Nikon).

Yeast Spotting Assays

Yeast were cultured in synthetic media consisting of 0.67% yeast nitrogen base without amino acids (Fischer Scientific) supplemented with amino acids (MP Biomedicals) and 2% sugar. Cells were first grown to mid-log phase in synthetic media containing glucose and then re-cultured overnight in synthetic media containing 2% raffinose. Mid-log phase cells were then diluted in synthetic media containing galactose. Typically, cells were induced for six hours at 30°C.Each strain was diluted to a starting OD_{600} = 1.0 and serially diluted 5-fold and then spotted on agar plates containing galactose (inducing) or glucose (control) plates.

QUANTIFICATION AND STATISTICAL ANALYSIS

The Quantification of the Membrane-2 Hybrid

In the membrane yeast two-hybrid assay, yeast growth phenotypes were scored as 1~4, based on the size of the growth spot, with 4 being the largest size. In the lenient interaction call, protein interactions were considered positive if both repeats got a score of 1 or more; in the stringent call, protein interactions were considered positive, if both scores were higher than 1, or at least one score was 4 and the other no lower than 1. In most analyses, stringent calls were employed for this study.

p Value for Figure 1 and Table 1

Bonferroni Adjusted p values were calculated by DAVID functional annotation clustering website, https://david.ncifcrf.gov.